EARTHQUAKE SPECTRA

The Professional Journal of the Earthquake Engineering Research Institute

PREPRINT

This preprint is a PDF of a manuscript that has been accepted for publication in *Earthquake Spectra*. It is the final version that was uploaded and approved by the author(s). While the paper has been through the usual rigorous peer review process for the Journal, it has not been copyedited, nor have the figures and tables been modified for final publication. Please also note that the paper may refer to online Appendices that are not yet available.

We have posted this preliminary version of the manuscript online in the interest of making the scientific findings available for distribution and citation as quickly as possible following acceptance. However, readers should be aware that the final, published version will look different from this version and may also have some differences in content.

The DOI for this manuscript and the correct format for citing the paper are given at the top of the online (html) abstract.

Once the final, published version of this paper is posted online, it will replace the preliminary version at the specified DOI.

Out-of-Plane Dynamic Stability of Unreinforced Masonry Walls in One-Way Bending: Parametric Study and Assessment Guidelines

Osmar Penner[1] and Kenneth J. Elwood[2], M.EERI

A numerical rigid body model for the out-of-plane response of unreinforced masonry (URM) walls connected to flexible diaphragms is validated against the shake table test results presented in a companion paper. It is demonstrated that the model is able to reproduce the observed rocking behaviour with reasonable accuracy, particularly the intensity of shaking resulting in collapse of the walls. The validated model is used to undertake a parametric study investigating the effects of numerous parameters on out-of-plane wall stability. Ground motion variability is accounted for by using a large suite of motions. Based on the results of the modelling, an updated out-of-plane assessment procedure is proposed. The procedure, which could be incorporated into ASCE 41, provides reference curves of h/t vs. $S_a(1.0)$, along with correction factors for axial load, wall thickness, ground-level walls, and exposure.

INTRODUCTION

As discussed in a companion paper, Penner and Elwood [2015], out-of-plane failures of URM walls during earthquakes constitute a significant life safety risk in many cities worldwide. A common procedure used to assess the collapse vulnerability of URM walls sufficiently anchored to diaphragms is included in ASCE 41-13. Based on original studies by ABK Joint Venture [1981], ASCE 41-13 (chapter 11) stipulates allowable h/t ratios as a function of the design spectral acceleration, S_a, at a period of 1 s and the wall's location in the building. While the ASCE 41 assessment procedure is used extensively in practice, it has numerous significant shortcomings. For example, axial load can vary significantly among top-storey walls, depending on the size of parapets and whether roof joists or trusses

[1]BC Hydro, 6911 Southpoint Drive, Burnaby, B.C. Canada V3N 4X8

[2]Dept. of Civil and Environmental Engineering, University of Auckland, 3 Grafton Road, Auckland, New Zealand

are bearing on the wall or running parallel to it, but the procedure does not distinguish between these cases. The effect of diaphragm flexibility is disregarded. The procedure assumes that wall stability is independent of scale effects, accounting only for the h/t ratio, but not for variation in wall thickness. In addition, despite having run the largest experimental campaign on one-way spanning walls to date, the data set on which the ABK Joint Venture assessment procedure was based was limited due to the lack of a numerical model. Ground motion variability was not accounted for, and the effects of parameters other than those varied in the experimental work were not considered. Recommended limits on h/t were arbitrarily reduced at various stages prior to incorporation in standards documents, with inadequate documentation.

Aside from hazard definition, no revisions have been made to the out-of-plane portion of the procedure since its inception, despite significant research progress having been made since ABK Joint Venture [1984]. The limitations of the original research and the following adaptations of its recommendations create uncertainty about the risk levels produced by the current standard. New research and modern computational power offer the ability to re-examine the out-of-plane response of URM walls far more thoroughly than before, with the potential to produce a new assessment procedure that better defines and controls the associated seismic risks. This paper extends the experimental study presented in the companion paper using a rigid-body rocking model to investigate factors influencing the out-of-plane response of URM walls and develop seismic assessment guidelines suitable for application in engineering practice.

NUMERICAL MODEL AND VALIDATION

Rocking behaviour as observed in the experimental study is best captured using a rigid-body mechanics model [Makris and Konstantinidis, 2003]. Similar to the study by Sharif et al. [2007], Working Model 2D [Design Simulation Technologies, Inc., 2010] was used to simulate the response of the wall-diaphragm system considering its well validated capability to simulate the pure sliding and pure rocking responses of a block subjected the seismic input [Konstantinidis and Makris, 2005].

The general configuration of the model, as used in the subsequent parametric study, is shown in Figure 1. The wall was modelled as two rigid bodies stacked one on top of the

other, resting on a frictionless base, representing the shake table. A rigid frame extends up from this base, representing the test frame. Spring-damper units connect this rigid frame to the top and bottom diaphragms (or carriages in the shake table tests). Each diaphragm was constrained to travel only horizontally. Spalling at the rocking interfaces (at the base and at the crack) was represented by assigning a chamfer to the appropriate corners of the wall bodies.

Consistent with the experimental setup described in Penner and Elwood [2015], the following modifications were made for the validation study:

1. no axial load was applied on the top of the wall;
2. a separate body fixed to the top of the wall was included to account for the mass and geometry of the top beam assembly;
3. the contact points at the bottom connection were located a short distance above the base of the wall to represent the rubber spacers; and,
4. chamfers at rocking interfaces were modelled at 45 degrees, with a leg dimension of 2 mm at the crack and 10 mm at the base of the wall, to best represent the observed damage at the crack and base.

The damping ratio for each carriage was defined in terms of the total spring constant for that carriage and the mass of the carriage plus half of the wall mass. For the validation study, the damping values were empirically calibrated to achieve a good fit to the measured carriage response for the larger oscillations. A damping ratio of 12 % was used for wall *FF-2*, and 8 % was used for all other walls. Dependence on wall size was considered appropriate since damping due to friction was dependent on the test specimen weight. A coefficient of restitution of 0.02 was assigned to both wall segments and kept constant in all analyses. Further details of the model implementation in Working Model are provided in Penner [2014].

Each run on the shake table in which the recorded table motion was applied to a cracked wall was simulated using the model. Since wall stability is fundamentally a displacement-governed problem, the displacement response is of primary interest in the validation of the model. In particular, the rocking response of the wall is the critical output, for which a prerequisite is accurate modelling of the response of the diaphragms.

Analogous to results from incremental dynamic analyses, the peak rocking displacements (normalized to the wall width) versus ground motion intensity are shown in Figure 2, with the modelled results overlaid in dashed blue lines. The model approximates the general trend of rocking displacements vs. motion intensity reasonably well. The collapse scale is very well simulated; the largest discrepancy is the premature simulated collapse of wall *FF-2* at 92% of the collapse scale factor from the shake table test. The minimal rocking of wall *FR-3* prior to the collapse run is well represented. There are some discrepancies in the peak rocking displacements observed in non-collapse runs, but this accuracy is considered adequate bearing in mind the objective of the study—to investigate the collapse capacity of URM walls.

Figure 3 illustrates the ability of the rocking model to reproduce the non-periodic rocking response. The time variation of the rocking motion is matched very well by the model, though the magnitudes of some of the rocking excursion peaks are smaller in the model than recorded in the test. In addition, the response of both the top and bottom carriages are matched exceedingly well for the entire duration of the run. Further comparison of the numerical and experimental results can be found in Penner [2014].

PARAMETRIC STUDY

Using the model described in the previous section, an extensive parametric study involving approximately 200 000 analyses was conducted to identify the most significant parameters influencing the out-of-plane stability of a URM wall anchored to floor diaphragms of varying stiffness. The model used for the parametric study was consistent with that shown in Figure 1. A reference configuration is described by the parameters in Table 1. The parametric study was conducted in several phases and included variations in the following parameters: diaphragm periods, wall thickness, h/t, crack height, spall depth at crack, diaphragm damping, diaphragm mass ratios, and axial load (magnitude and location of load application). The following sections focus on the results most pertinent to the development of new assessment procedures; a full description of the results of the parametric study can be found in Penner [2014].

In considering the parameters of the parametric study, it is worth reflecting on the definition of the 'diaphragm period' (T_b or T_t). A cracked wall connected to flexible diaphragms

combines three responses: the vibration of two diaphragm systems and the rocking response of the wall. The diaphragm period, as defined here using half the mass of the wall and the mass of the diaphragm, is a reference indicator of diaphragm stiffness, and is an approximation of the initial period of vibration of a diaphragm connected to uncracked walls. As observed in Penner and Elwood [2015], the rocking motion of a cracked wall does not have a distinct period. Furthermore, the additional degree of freedom created by the crack changes the effective mass of the diaphragm system, thereby changing its effective period relative to that calculated by assignment of tributary mass. While the diaphragm period is a convenient and intuitive way to characterize such a system, it is important to keep note of its limitations.

Ground motions recommended in FEMA P695 [FEMA, 2009] were used for the parametric study. Portions of the study were run using the full set of motions, including the near-fault motions, though the analysis described herein focuses primarily on the far-field set (44 records). Rocking response, and hence stability, of URM walls was found to be highly dependent on ground motion. It is noted that ABK Joint Venture [1981], the reference primarily responsible for the current out-of-plane assessment procedures in ASCE 41, used only four ground motions. The consideration of a large set of ground motions in the current study and development of new assessment procedures is considered an important contribution.

INTENSITY MEASURE

For any single model configuration, each ground motion was incrementally scaled until collapse of the wall was observed. The primary interest in the analysis of the results lies in quantifying the intensity of the motions that result in collapse. Once the analysis is complete, each motion's scale at the lowest level causing collapse is known, and it remains to describe the intensity of these motions. Many possible intensity measures could be used — e.g., peak ground acceleration/velocity/displacement, spectral acceleration/velocity/displacement at a period of choice, Arias intensity, etc. As a starting point, the acceleration response spectrum of each ground motion at the scale causing collapse was compiled. The distribution of spectral values at each period increment was evaluated, as shown in Figure 4 for the reference configuration. A cumulative distribution function (CDF) for the probability of collapse (P_{col}), or fragility curve, can be determined by integrating the probability density function illustrated in Figure 4 (examples of fragility curves

are shown in Figures 7–9). A lognormal distribution was found to provide an excellent fit to results throughout the parametric study.

One approach to quantifying the appropriateness of an intensity measure is to consider the variability produced in the fragility curve using that intensity measure. Tightly distributed results—exhibiting less variance (steeper fragility curves)—are preferable to results exhibiting larger variance, in the sense that it is undesirable to use an intensity measure that introduces additional variance simply because the measure is uncorrelated to the response quantity of interest. A low variance suggests that the selected measure is in fact closely correlated to the response quantity. The coefficient of variation (c_v) is a convenient indicator of this variance, since it is normalized to the mean of the distribution.

Figure 5 shows the c_v for $S_a(T_{im})$, where T_{im} denotes the period at which the intensity measure is taken, for model configurations with different system periods (such that $T_t = T_b$, denoted simply as system period, T_s). Several noteworthy features can be observed. First, all configurations with system periods of 0.75 s or longer feature similar sharp minimums of c_v at $T_{im} = T_s$, and the minimum c_v values are similar for each of these configurations. For configurations with shorter periods, however, there is no well-defined minimum of c_v at any T_{im}. Second, configurations with system periods of 1.25 s or longer exhibit considerably larger variance for small T_{im} than those systems with periods of 1.0 s or shorter. Examining the trends in this plot suggests that the choice of $T_{im} = 1.0\,\mathrm{s}$ produces close to the lowest overall variance among systems with periods varying between 0 and 2 s. Long period systems are subject to the highest variance with this selection. For the systems with periods of 0, 0.2, and 0.5 s, this selection actually yields close to the lowest possible variance - better than at $T_{im} = T_s$.

Spectral acceleration is a universal design parameter readily available to practicing engineers, which makes it a logical choice for selection as an intensity measure. In addition, $S_a(1.0\,\mathrm{s})$ specifically is typically a key benchmark within a design spectrum. It is also the parameter used by the existing assessment procedure for out-of-plane stability of URM walls in ASCE 41 [ASCE, 2013]. Combined with the results of Figure 5 discussed previously, these factors form a strong case for the selection of $S_a(1.0\,\mathrm{s})$ as the intensity measure of choice, and it will be used in the sections that follow.

DIAPHRAGM STIFFNESS

Configurations with equal top and bottom periods between 0 (rigid) and 2 s are considered. Figure 6 shows constant P_{col} points for 10% and 50% levels. At a given period, the difference between the two curves indicates the variance of the fragility curve for that period. Variance is smallest at $T_s = T_{im} = 1.0\,\text{s}$, is larger but reasonably consistent for shorter periods, and increases more significantly towards longer periods — consistent with Figure 5. Due to the discrepancies in variance among the various periods, the 50% curve is perhaps most representative of the 'real' trend in this figure. Walls in systems where $T_s \leq 0.2\,\text{s}$ are significantly more stable than those with longer periods. Stability increases once more at periods beyond 1.25 s. Stability is lowest at $T_s = 0.75\,\text{s}$, but not much lower than at other points between 0.5 and 1.25 s. The higher variance for long period systems, however, raises concerns regarding relying on the increased stability as the diaphragm period increases beyond 1.25 s.

The configurations considered in Figures 4–6 all assume the top and bottom diaphragm periods are the same. In reality, diaphragms are likely to vary in stiffness, particularly in the top storey where one diaphragm is a roof while the other is a floor. The top and bottom inputs into the out-of-plane wall can thus be out of phase, which has the potential to change the response significantly. Figure 7 shows the fragility curves for all four combinations of periods of 0.5 and 1.0 s distributed between the top and bottom of the wall. The configurations with equal top and bottom periods bracket the responses, with the varying top and bottom periods falling in between. A similar trend is observed for other combinations of top and bottom periods.

In general, it can be concluded that the out-of-phase action produced by diaphragms of different stiffness at the top and base of a wall will result in out-of-plane wall stability in between that of configurations when both diaphragms are equal to one of these periods. Typically there is significant uncertainty in the assessment of diaphragm periods, and it would not be prudent to rely on a calculated difference in period to produce an increase in assessed wall stability. For a given wall, it would be reasonable to use the least stable of the two calculated periods at the top and bottom when conducting an assessment.

It is critical to clarify that the term *stability*, in this study, refers to the aggregated collapse levels of a sufficiently large suite of ground motions, i.e. the entire fragility curve.

The conclusions do not necessarily hold for any single ground motion, where the stability at various periods is dependent on the distribution of peaks and valleys in the response spectrum. For fragility curves of systems with different periods, one cannot assume that each ground motion falls at the same location on each curve—in fact, it is unlikely. Comparisons of these analysis results with the test results from Penner and Elwood [2015] must therefore be made cautiously. Because the tests used only a single ground motion, the fact that wall *FR-3* performed better than both *FF-3* and *RR-3* can still be considered consistent with the analysis results bearing in mind the close match between experimental and numerical results shown in Figure 2.

SLENDERNESS RATIO AND THICKNESS

Walls of constant thickness and varying height were evaluated, where slenderness ratios varied between 4 and 22. Fragility curves are plotted in Figure 8. As expected, more slender (taller) walls consistently exhibited lower stability than less slender (shorter) walls. Variance is fairly consistent among the distributions, with the exception of the curve at $h/t = 4$, which shows notably more variance than the others.

Walls with the same slenderness ratio ($h/t = 11$) but different thicknesses (and therefore heights) were evaluated. The thicknesses were representative of typical one-, two-, and three-wythe walls: 110, 220 and 330 mm, respectively. The fragility curves for $T_s = 1.0$ s are plotted in Figure 9. Consistent with Sorrentino et al. [2008], thinner walls exhibited consistently lower stability than thicker walls with the same slenderness ratio. Similar results are observed for different system periods and h/t.

AXIAL LOAD

The details of how axial load is applied result in very significant differences in its effect on stabilization of the rocking response. Five specific cases for load application were considered, as illustrated in Figure 1.

- An applied force at a fixed location: (1) at the wall centerline, and (2) at $0.4 \cdot t$ away from the centerline.
- A load applied to a block that remains horizontal, where the block starts at one edge of the wall below and extends across the wall thickness by (3) one wythe, (4) two wythes, and (5) three wythes.

Cases 1 and 2 may be considered representative of load from prestressing; Case 3: a joist pocket on a 3-wythe wall; Case 4: a braced 2-wythe parapet on top of a 3-wythe wall; Case 5: load from an upper story wall. Constant P_{col} values are plotted in Figure 10 for all 5 cases for a range of typical axial load levels, including the best-fit straight lines (constrained through $S_a(1.0) = 0.3\,\mathrm{g}$ at zero load). The greatest stability gains for a given load are produced by Case 5, followed by Case 4. Case 3 produced nearly the same effect as Case 1. The effects of axial load are the result of a combination of the effects in each of the two possible rocking directions. In every case, the axial load is stabilizing until the rotation of the top wall segment becomes such that the contact point between the top and bottom wall segments is directly below the point of action of the axial load on the top block. For Case 2, this rotation limit is very small in one direction, resulting in the smaller stability gains with axial load for this case.

Note that the capacity gets very high for non-top storey walls (Case 5), consistent with the lack of out-of-plane failures in lower stories observed in past earthquakes. With one storey above, overburden loads could be expected to be in the range of 20–50 $\mathrm{kN/m}$.

To further illustrate the importance of overburden, Figure 11 shows the $S_a(1.0\,\mathrm{s})$ at a $P_{col} = 10\%$ for varying periods and h/t for the cases of zero axial load and $p = 10\,\mathrm{kN/m}$ (ASCE 41 limits are also included for reference). The overburden was applied entirely as joist pocket loading (Case 3). Figure 11a and Figure 11b illustrate that the magnitude of the effect of the diaphragm period is heavily dependent on the slenderness ratio, with the effect being more important for less slender walls with axial load. It is clear that the $T_s = 0$ configuration consistently results in the highest stability, with the $T_s = 0.5\,\mathrm{s}$ configuration remaining at notably lower stability levels even as the axial load increases. For $p = 10\,\mathrm{kN/m}$ (Figure 11b), the $T_s = 2.0\,\mathrm{s}$ configuration reaches the same level of stability as the stiff systems.

Figure 11c illustrates stability gains with application of overburden by considering the ratio of S_a with overburden to S_a without overburden at P_{col}= 10%, for variations in h/t and T_s. Linear regressions for constant values of T_s are included. This plots demonstrates that the stabilizing effect of overburden depends heavily on h/t, with greater relative stability gains occurring for smaller h/t.

GROUND FLOOR WALLS

Figure 12 compares the stability of a wall connected to two flexible diaphragms to that of a wall connected to a flexible diaphragm at the top and a rigid diaphragm at the base (representative of a one story building where the rigid diaphragm is the ground level). It can be noted that the slenderness ratio has minimal influence overall on the effect of fixing the bottom diaphragm. The period has notable influence, however, with the greatest stability gains occurring at $T_s = 0.5\,\mathrm{s}$. For the most part, making the bottom diaphragm rigid results in mild stability gains. This is consistent with earlier observations of systems with mixed top and bottom periods exhibiting stability in between that at either period.

FURTHER CONSIDERATIONS

Moving from the results of the parametric analysis to the development of an assessment procedure involves simplifications and the subjective evaluation of numerous factors not directly considered in the parametric study. In this section, principal factors relevant to the development of assessment guidelines are discussed.

DIAPHRAGM DISPLACEMENTS

Results in previous sections have been presented in terms of spectral accelerations, in large part because this is the most common design criterion used in practice. When dealing with long-period diaphragms, where displacements resulting from a given spectral displacement can be large, it is important to maintain an awareness of deformation compatibility. Diaphragm deformations at moderate S_a values are less than roughly half the thickness of a three-wythe wall for systems with diaphragm periods up to roughly 1 s, assuming that the linear response of a system with a secant stiffness is representative of the actual response of the diaphragm (e.g., at $S_a(1\,\mathrm{s}) = 0.6\,\mathrm{g}$, $S_d(1\,\mathrm{s}) \approx 150\,\mathrm{mm}$). At periods much beyond this, deformations increase rapidly, since S_d is proportional to T^2. Large deformations, particularly if occurring in buildings with short diaphragm spans, can cause deformation compatibility issues not directly related to out-of-plane wall failure, such as vertical wall cracks due to horizontal bending and damage at corners and cross walls.

The results presented in the parametric study indicate that the large displacements associated with long-period systems do not create a higher risk of collapse within the limitations

of the one-way rocking model. Despite this, in light of the potential deformation compatibility issues associated with large diaphragm deformations, it would be prudent to make assessment guidelines increasingly conservative as diaphragm periods increase.

RESPONSE ALONG THE DIAPHRAGM

The diaphragm response varies significantly along its length. Disregarding two-way effects, one could conservatively imagine an out-of-plane wall along the span of a diaphragm as a series of tall and narrow one-way spanning strips. This concept is illustrated in Figure 13, which shows a single wall with window perforations connected to flexible diaphragms at top and bottom. The wall strips in the illustration are cracked and undergoing rocking. The strips near the ends of the diaphragm would be subject to the equivalent of a rigid diaphragm input, while the strips at the diaphragm centerline would be subject to a relative diaphragm response approximately 1.27 times that of the equivalent SDOF model used in this study [Penner, 2014]. Not only would the inputs to the wall strips at the other points along the span be different, but the resulting differences in wall rocking response would also affect the response of the rest of the diaphragm. Neither of these effects was accounted for within the scope of the present study.

Given that the parametric study showed that stiff and rigid diaphragm systems resulted in the highest out-of-plane stability, it is unlikely that points of intermediate response between the equivalent SDOF system and the rigid system would produce lower stabilities. In particular for short-period diaphragms, it is possible that the wall strips at mid-span would result in lower stability than the SDOF system modelled due to the larger diaphragm deformations at this location. Whether additional conservativeness beyond the modelled results is necessary to account for this effect may be a matter of opinion, but the effects of two-way bending, as described in the next section, would in many cases provide some reserve resistance.

TWO-WAY BENDING AND WALL GEOMETRY

Griffith et al. [2007] conducted cyclic air bag testing of two-way supported URM wall panels. They showed that the addition of vertical supports at the ends of wall panels resulted in significant additional reserve displacement capacity beyond that available through one-way bending. In this same study, however, it was noted that a large proportion of vertical cracking was due to line failure (cracking through bricks) rather than stepped failure

(cracking at the brick–mortar interface). While "stepped cracks can possess significant reserve post-cracking moment capacity due to the torsional resistance from friction acting on the bed-joints", line cracks can not [Griffith et al., 2007]. In the most extreme cases, full-height line cracks can effectively completely negate two-way bending effects.

Full-scale dynamic testing of two-way supported wall panels has not been carried out to date (except infill panels supported by a stiff concrete frame), and the existing work does not clearly conclude how much additional dynamic stability is achieved by two-way supports vs. one-way supports. Two-way effects appear unlikely to be detrimental to dynamic stability, however the demonstrated potential for line cracking necessitates caution in incorporating any benefits from two-way bending into assessment guidelines. Due to these issues, two-way effects were conservatively ignored in the derivation of guidelines.

In addition to two-way effects, other geometry issues can complicate wall assessment. Notably, gable end walls have continuously varying heights along their length, and the relationship between their dynamic stability and that of a constant-height wall is unclear. Both of these topics are of interest for future research.

AMPLIFICATION UP THE BUILDING

There is very limited research available on the amplification of ground motions up the height of URM buildings. ABK Joint Venture [1981] ignored the issue entirely by rationalizing that between foundation rocking and non-linearity of URM in-plane response it was unlikely that accelerations would be greater at the top of a building than at the base. However, one available instrumentation record in a real building revealed notable amplification [Tena-Colunga and Abrams, 1995], particularly at short periods, and recent modelling [Knox, 2012], while not exhaustive, certainly suggested that some amplification may be likely. Menon and Magenes [2011a,b] conducted a parametric study on amplification effects in URM buildings with rigid diaphragms; although the global response is expected to differ significantly from buildings with flexible diaphragms, it was noted that significant amplifications up the height of the building are possible.

Through the assessment of a relevant intensity measure (Figure 5), the present study has demonstrated that out-of-plane wall stability—for both rigid and flexible diaphragm systems—is more dependent on long-period input motion content than short-period content. Short period amplification of input motions would therefore not be expected to cause

significant changes in wall stability, and the use of the results of the current study, which used unamplified ground motions as input to diaphragms, is considered reasonable. Further research on this topic may serve to validate this assumption in the future.

ARCHING ACTION

Derakhshan et al. [2014] found during in-situ airbag testing of URM walls in vintage buildings that the effect of arching action provided by timber roof diaphragms was negligible. Other construction details, such as concrete ring beams, can provide notable arching action effects substantially improving wall stability; however, such effects have not been demonstrated in dynamic testing.

An approximation of arching action could be rationalized based on the effects of axial load demonstrated in the parametric study by calculating the vertical stiffness of the support and the increase in height of the wall during rocking. It would be expected that the effect would be less than that due to an axial load corresponding to the maximum force predicted due to the arching, since arching resistance is only mobilized as the wall rocking displacement increases. Regardless, excluding the effect is conservative in all cases, and for flexible timber diaphragms it is in fact accurate.

MASONRY STRENGTH

Meisl et al. [2007] showed that the quality of collar joints in multi-wythe walls had little effect on their out-of-plane response during dynamic testing. However, vintage URM construction may exhibit considerably weaker mortar than that used during testing (e.g., Lumantarna et al. [2014]), in terms of both flexural bond strength and mortar compressive strength. After initial cracking, mortar strength may influence the integrity of the wall at the crack considering the impacts associated with rocking, but otherwise wall stability is not expected to be heavily influenced by mortar strength. While wall segments in the current tests sustained negligible damage outside of the characteristic horizontal cracks, it is not clear how well vintage masonry with very low strength mortar would hold together under sustained rocking behaviour. Low-strength walls tested by Wilhelm et al. [2007] exhibited significant cracking under dynamic loading; however, limited experimental work on this topic is available. The modelling in the current study included the effects of moderate amounts of spalling at the crack location. While this modelling approach is considered adequate for the development of assessment guidelines, it may be prudent not to rely on

rocking stability for walls with extremely low mortar strengths where wall integrity may be compromised by impacts at the cracks.

Additionally, masonry strength can be a consideration for anchorage design. A recent anchor-testing program conducted in New Zealand showed anchor capacity to be dependent on masonry strength, but also that properly-installed anchors can still function adequately in low-strength walls [Dizhur et al., 2013]. Provisions for adequate anchoring in low-strength walls should be carefully considered along with those for out-of-plane stability.

DAMPING AND NON-LINEARITY

Assumed damping values have a moderately significant effect on out-of-plane stability [Penner, 2014]. A consensus on appropriate damping ratios for timber diaphragms in real buildings has yet to be reached. Wilson [2012] suggested a value of 5% may be appropriate, while in-situ testing by Giongo et al. [2015] indicated values of 10 to 30% may be more realistic. This study adopts the more conservative and traditional value of 5%.

Diaphragm non-linearity was not accounted for in this study. The diaphragm stiffnesses on which the period ranges were based were approximating secant stiffnesses at 100 mm deformation. The tested response characteristics [Wilson, 2012] would suggest that stiffness degradation beyond this point is likely to be minor. In addition, the reduced input accelerations that would result from non-linearity would be unlikely to reduce wall stability.

IN-PLANE DAMAGE

Perhaps the most significant simplification in the current study (and in most previous work on the topic) is that it considers out-of-plane wall response independently of in-plane response. In reality, all walls in a building are both ‘out-of-plane walls’ and ‘in-plane walls’ simultaneously when subjected to an actual earthquake. It can be argued that this issue is not of significant importance since in-plane damage tends to be concentrated in lower floors where in-plane demands accumulate, while out-of-plane failures tend to occur in the top floor, where axial load is lowest. Furthermore, Gülkan et al. [1990] and Clough et al. [1990] noted in shake table testing of one-storey masonry houses that minimal differences in response were observed when testing with three-axis input versus one-axis input. Nonetheless, future dynamic tests considering the influence of in-plane damage are encour-

aged.

VERTICAL ACCELERATIONS

The effect of vertical accelerations on the out-of-plane stability of URM walls, is beyond the scope of this study. The fact that out-of-plane response depends heavily on the axial force on the wall suggests that vertical effects could be important. On the other hand, the high-frequency nature of the vertical excitation means that several full cycles of vertical motion may occur during a single rocking excursion, which may in the end result in minimal overall difference. At this point, the issue is unresolved, and merits further research.

ACCEPTABLE RISK LEVEL

It is proposed that variation in risk levels could be considered among different wall specimens of the same building based on an assessment of the exposure. In the context of out-of-plane wall failure, the greatest life safety risk is due to wall debris falling onto an occupied street or sidewalk, rather than precipitating total building collapse. Moon et al. [2014] noted during a post-earthquake survey of URM damage in Christchurch that walls and gables are significantly more likely to fall outwards from a building than inwards due to restraint from the diaphragms, resulting in a larger life safety risk for nearby pedestrians than for building occupants. URM buildings with light timber diaphragms frequently have enough redundancy to maintain support for the light floor and roof structures, thereby protecting occupants, despite out-of-plane wall failures (Figure 14).

Consider as an example the top storey of a two-storey commercial URM building, with the façade located on a busy pedestrian street and roof joists supported on the front and back walls. Out-of-plane failure of the front wall in the daytime has the potential to cause significant loss of life, both for pedestrians on the ground in front of the building, and for occupants of the top storey since the roof is supported on this wall. In comparison, out-of-plane failure of a side wall has much lower potential to cause loss of life, since the area below (say, an alley) is less likely to be occupied, and this wall is not integral to the support of the roof. While the conservative (and simple) solution would be to apply the same assessment standards to both of these walls, in the context of a limited retrofit budget, a greater overall risk reduction would be achieved by applying a higher standard to the high-risk front wall and a lower standard to the low-risk side wall. To this end, it is proposed

to add an 'exposure factor' to the out-of-plane wall assessment procedure described in the following section.

RECOMMENDATIONS FOR ASSESSMENT GUIDELINES

In this section, an out-of-plane wall assessment procedure is proposed as an update to the current procedure in ASCE 41-13 based on the results of the parametric study and the discussion in the previous section. The proposed procedure is considered to yield an assessment at the collapse prevention (CP) performance level, as does the current procedure. The recommended procedure is summarized as follows, with subsequent sections providing more details regarding each step.

- Classify diaphragms as stiff or flexible
- Obtain the corresponding base curve of $S_{a_b}(1)$ vs. h/t
- Obtain a correction factor for axial load, C_a
- Obtain a correction factor for wall thickness, C_t
- Obtain a correction factor for exposure level, C_e
- Obtain a correction factor for ground level walls, C_g
- Compute the final relationship for allowable $S'_a(1) = C_a \cdot C_t \cdot C_e \cdot C_g \cdot S_{a_b}(1)$

BASE CURVES AND CLASSIFICATION OF DIAPHRAGMS

The parametric study showed that very stiff and rigid diaphragms resulted in the most stable walls, while mid-range periods resulted in considerably lower stability. Very long periods showed some improvement over mid-range periods. It is recommended that diaphragm flexibility classification be limited to two categories—stiff ($T_s < 0.2$ s) and flexible ($T_s > 0.5$ s)—along with a transition range between the two. Allowing more detailed classification of flexible diaphragms is not recommended for two reasons: (1) there is significant uncertainty in assessing diaphragm periods, and (2) allowing benefits for longer periods is not prudent due to deformation compatibility issues that may arise with the larger deformations of long-period systems.

The base curves for each case are defined for no axial load, at $P_{col} = 10\%$, in 3-wythe walls in upper stories. For each classification, the base curves are selected to approximate the parametric study results for the most conservative periods: ($T = 0.2$ s for stiff systems,

and $T = 0.5\,\text{s}$ for flexible systems). In the transition range, the base curve can be linearly interpolated based on the system period. The recommended relationships, Equation (1), are plotted in Figure 15 against the relevant results from the parametric study and the current ASCE 41 limits. The base curve for stiff diaphragms is reasonably consistent with current ASCE 41 limits for top storey walls, at low h/t, and with the limits for one storey walls, at higher h/t. The base curve for flexible diaphragms is notably more conservative than current ASCE 41 limits and the base curve for stiff diaphragms (approximately 2/3 of allowable Sa for flexible diaphragms at h/t=10), in accordance with the findings of this study.

$$S_{a_b}(1) = \begin{cases} 4 \cdot \left(\frac{h}{t}\right)^{-1} & \text{stiff diaphragms } (T_s < 0.2\,\text{s}) \\ \frac{3}{2} \cdot \left(\frac{h}{t}\right)^{-\frac{3}{4}} & \text{flexible diaphragms } (T_s > 0.5\,\text{s}) \end{cases} \quad (1)$$

CORRECTION FACTORS

The base curves must be adjusted to account for the effects of axial load, wall thickness, exposure level, and whether walls are at ground level or in an upper storey. Correction factors for each of these effects are presented below.

Axial load

Axial load on a wall can significantly improve its stability, with Figure 10 suggesting that the relative stability gains increase with increasing load. Considering a joist pocket loading (onto the outer wythe of a 3-wythe wall), the modelling results further indicate that stability gains due to axial load decrease with increasing h/t (see Figure 11c). Results varied significantly for different periods, and again the most conservative points are at $T = 0.2\,\text{s}$ for stiff systems, and $T = 0.5\,\text{s}$ for flexible systems. It may be prudent not to rely heavily on axial load gains due to possible countering effects from vertical accelerations. Wall response under simultaneous horizontal and vertical input motion was outside the scope of this study, and further study is required in this area.

The following formulation is recommended for the axial load correction factor, C_a:

$$C_a = \begin{cases} 1 + C_a' \cdot \left(\dfrac{p}{10}\right) & \dfrac{h}{t} < 8 \\ 1 + C_a' \cdot \left(\dfrac{p}{10}\right)\left(1 - \dfrac{1}{12}\left(\dfrac{h}{t} - 8\right)\right) & 8 \leq \dfrac{h}{t} \leq 20 \\ 1 & \dfrac{h}{t} > 20 \end{cases} \quad (2)$$

Here, p is in kN/m and C_a' is defined as 0.5 for stiff diaphragms and 0.2 for flexible diaphragms. The value of C_a' for systems in the transition range can be linearly interpolated based on the system period. While the modelling results suggest that these relationships should remain valid even at large p, it is recommended to implement a cap at $p = 20\,\text{kN/m}$ to avoid excessive stability gains. C_a values are plotted for $p = 10$ and $20\,\text{kN/m}$ in Figure 16; the curves agree with modelling results for $T = 0.2\,\text{s}$ and $T = 0.5\,\text{s}$ from Figure 11c (for $p = 10\,\text{kN/m}$). Notably, very slender walls are not allocated stability benefits from axial load.

Wall thickness

Past research [Makris and Konstantinidis, 2003] and results from the parametric study indicate that for a given aspect ratio, rocking stability is greater for larger bodies than for smaller ones. This is reflected in the recommended correction factor for wall thickness, Equation (3). As shown in Figure 17, this correction factor is generally conservative relative to results from the parametric study.

$$C_t = 0.2 + \frac{5}{2} \cdot t \leq 1.0, \; t \text{ in m} \quad (3)$$

Exposure

As discussed previously, it is of interest to account for varying levels of risk corresponding to higher or lower exposure conditions. An exposure factor, C_e, is proposed that accounts for variations from the base curve case, with $P_{col} = 10\%$, according to the assessed exposure for a particular wall. The assessment should take into account the wall's role in the support of the structure's gravity system, and the likelihood of occupants being located in the impact zone in the case of wall failure. In regards to the latter, it has been shown to be far more common for debris from out-of-plane wall failures to fall outward than inward [Moon et al., 2014]; as such, assessment emphasis should be placed on the

exposure outside the building. The base case of $P_{col} = 10\%$ is deemed to be a reasonable risk level for default high-risk conditions. It is recommended to define C_e as approximating the differences between P_{col} values from the parametric studies, as listed in Table 2. These values were derived by comparing results such as those shown in Figure 11b for different probabilities of collapse at $T = 0.2\,\mathrm{s}$ for stiff systems and $T = 0.5\,\mathrm{s}$ for flexible systems. The value of C_e for systems in the transition range can be linearly interpolated based on the system period.

The definition of what constitutes each level of exposure should be carefully considered. In particular, the 'very low' case defined here should be used only under stringent conditions. Note that the study used as a basis for these results considered only the uncertainty in the wall response. A complete risk study should include the uncertainty in both the hazard and the exposure before any decisions are made regarding adopting specific factors.

Ground level

In flexible diaphragm systems, modelling results showed mild stability gains for walls in which the base was connected to a rigid diaphragm (e.g., for a one-storey building) vs. those connected to flexible diaphragms at top and bottom (upper storey walls) — see Figure 12. While these results showed negligible stability gains at very long periods (2 s), the simplifications made in the definition of the base curves (Figure 15) left reserve capacity at these periods, making it reasonable to apply constant stability gains at all periods. These gains can be accounted for by applying a ground level correction factor, C_g, defined as follows:

$$C_g = \begin{cases} 1.0 & \text{stiff diaphragms} \\ 1.1 & \text{flexible diaphragms} \end{cases} \tag{4}$$

The value of C_g for systems in the transition range can be linearly interpolated based on the system period.

SAFE SEISMIC HAZARD LEVEL

The ASCE 41 special procedure specifies that out-of-plane stability need not be evaluated for sites at which $S_a(1) \leq 0.133$, where S_a is the spectral acceleration for the hazard level adopted for the CP performance level. This lower bound is re-evaluated using the new

procedure. Conservative conditions are chosen to represent worst-case walls connected to flexible diaphragms: $t = 200\,\text{mm}$ represents two-wythe walls, and walls are assumed to be in the top storey with no axial load and very high exposure. At $h/t = 26$, this produces an allowable $S'_a(1)$ of 0.08 g.

It can be concluded that at sites with a hazard level of $S_a(1\,\text{s}) \leq 0.08\,\text{g}$, out-of-plane stability need not be evaluated for URM walls that meet all of the following criteria:

- have a thickness of at least 200 mm,
- are adequately anchored to the diaphragms at all levels, and
- are within reasonable h/t bounds bearing in mind stability issues under gravity loads.

EXAMPLE

The proposed assessment procedure is applied to an example building to demonstrate differences with ASCE 41. Consider the front walls of a large two-storey commercial building. The building has three-wythe walls in both levels, and a 1.5 m tall parapet on the front. The building is $16 \times 24\,\text{m}$ in plan, with vintage single-sheathed wooden diaphragms classified as flexible. The front walls are bearing a 2.5 m tributary width of diaphragm weight. The walls' exposure has been assessed as high risk. The resulting assessment curves from the proposed procedure for the existing building are shown as solid lines in Figure 18, along with the limits for walls in multi-storey buildings from ASCE 41. The proposed curves are similar to the most conservative points on the ASCE 41 limits around $h/t = 9$ for the top storey and around $h/t = 18$ for the first storey. At other h/t values, the new curves are more conservative than the current limits.

Two possible retrofits for the example building are considered: (A) adding a plywood overlay to the existing diaphragms, and (B) pouring a 100 mm thick concrete slab on top of the existing diaphragms. It is assumed for this example that both retrofits will result in a 'stiff' diaphragm classification. For retrofit A, the added self-weight is considered negligible. For retrofit B, the total self-weight of the retrofitted diaphragms is assumed to be $2.5\,\text{kN/m}^2$. The assessment curves for the retrofitted building are shown as dashed lines in Figure 18. It is apparent that the retrofitted building is allowed significantly higher demands on out-of-plane walls than the existing building. In the top storey, the proposed

curves compare well with the least conservative point in the current standard, while in the bottom storey, the new curves are representative of the middle range of the ASCE 41 limits. The additional axial load for retrofit B slightly increases the stability of the top storey, whereas in the bottom storey the maximum allowable stability increase due to axial load had already been mobilized prior to the retrofit. For this example, the effect of stiffening the diaphragms is much larger than that due to the addition of self-weight.

CONCLUSIONS

A new method for the assessment of out-of-plane wall stability has been developed based on the conclusions drawn from an extensive parametric study. Key aspects of the model, including the wall response under varying diaphragm flexibility, were calibrated to the results of shake table testing. The parametric study demonstrated that stability of URM walls improves for:

- decreasing h/t,
- increasing axial load (while the extent of increase is greater for squat walls than for slender walls),
- increasing wall thickness,
- ground stories for buildings with flexible diaphragms, and
- stiff diaphragms relative to flexible diaphragms.

The new assessment method recommended in this study is a significant change from the procedure in the current ASCE 41 standard. For flexible diaphragm systems, the new method tends to be more stringent than the current standard; in some cases, significantly so. For stiff diaphragm systems, the new method tends to be consistent with the current standard. While there remains significant room for refinement and additional research, the method presented here offers significant improvements over the current method in terms of risk consistency among varying wall configurations, and by providing a thorough rationale for its details based in numerical and experimental work.

Several additional considerations are noteworthy in the process of implementing potential changes to the current assessment standard. The current ASCE 41 limits cut off allowable h/t values at maximum values. Results from the current study do not objectively

support an h/t cut-off based purely on the stability of the one-way rocking model. While wall heights and h/t values are already effectively limited by construction practices, general prudence and engineering judgement may favour applying hard limits in the assessment procedure.

Finally, considering the variability in collapse performance in the parametric study, the definition of base curves and correction factors in these recommendations erred towards conservativeness, most prominently so in flexible diaphragm portions. The notable variance in modelling results with varying system period resulted in systems with periods of 0.5 s typically governing the definition of parameters. Particularly in regards to the axial load effect, these values were significantly more conservative than at longer periods. The subjectivity inherent in the choice of parameter values may well allow for more relaxed selections in certain cases. A model, such as that developed herein using Working Model 2D, could potentially be used to evaluate specific conditions where relaxation of the proposed provisions is considered appropriate.

REFERENCES

ABK Joint Venture (1981). "Methodology for mitigation of seismic hazards in existing unreinforced masonry buildings: Wall testing, out-of-plane." *ABK Topical Report 04*, National Science Foundation, El Segundo, California.

ABK Joint Venture (1984). "Methodology for mitigation of seismic hazards in existing unreinforced masonry buildings: The methodology." *ABK Topical Report 08*, National Science Foundation, El Segundo, California.

ASCE (2013). "Seismic evaluation and retrofit of existing buildings." *ASCE 41-13*, Reston, VA, USA.

Clough, R. W., Gülkan, P., Manos, G. C., and Mayes, R. L. (1990). "Seismic testing of single-story masonry houses: Part 2." *Journal of Structural Engineering*, 116(1), 257–274.

Derakhshan, H., Dizhur, D., Griffith, M. C., and Ingham, J. M. (2014). "In situ out-of-plane testing of as-built and retrofitted unreinforced masonry walls." *Journal of Structural Engineering*, 140(6), 04014022.

Design Simulation Technologies, Inc. (2010). *Working Model 2D User Guide*. Version 9.0.3.806.

Dizhur, D., Campbell, J., Schultz, A., and Ingham, J. (2013). "Observations from the 2010/2011 canterbury earthquakes and subsequent experimental pull-out test program of wall-to-diaphragm adhesive connections." *Journal of the Structural Engineering Society New Zealand*, 27(1), 11–20.

FEMA (2009). "Quantification of building seismic performance factors." *FEMA P695*, Washington, D.C., USA.

Giongo, I., Dizhur, D., Tomasi, R., and Ingham, J. M. (2015). "Field testing of flexible timber diaphragms in an existing vintage URM building." *Journal of Structural Engineering*, 141(1), D4014009.

Griffith, M. C., Vaculik, J., Lam, N. T.-K., Wilson, J., and Lumantarna, E. (2007). "Cyclic testing of unreinforced masonry walls in two-way bending." *Earthquake Engineering & Structural Dynamics*, 36(6), 801–821.

Gülkan, P., Clough, R. W., Mayes, R. L., and Manos, G. C. (1990). "Seismic testing of single-story masonry houses: Part 1." *Journal of Structural Engineering*, 116(1), 235–256.

Knox, C. L. (2012). "Assessment of perforated unreinforced masonry walls responding in-plane." Ph.D. thesis, University of Auckland, New Zealand.

Konstantinidis, D. and Makris, N. (2005). "Seismic response analysis of multidrum classical columns." *Earthquake engineering & structural dynamics*, 34(10), 1243–1270.

Lumantarna, R., Biggs, D. T., and Ingham, J. M. (2014). "Compressive, flexural bond, and shear bond strengths of in situ New Zealand unreinforced clay brick masonry constructed using lime mortar between the 1880s and 1940s." *Journal of Materials in Civil Engineering*, 26(4), 559–566.

Makris, N. and Konstantinidis, D. (2003). "The rocking spectrum and the limitations of practical design methodologies." *Earthquake engineering & structural dynamics*, 32(2), 265–289.

Meisl, C., Elwood, K., and Ventura, C. (2007). "Shake table tests on the out-of-plane response of unreinforced masonry walls." *Canadian Journal of Civil Engineering*, 34(11), 1381–1392.

Menon, A. and Magenes, G. (2011a). "Definition of seismic input for out-of-plane response of masonry walls: I. Parametric study." *Journal of Earthquake Engineering*, 15(2), 165–194.

Menon, A. and Magenes, G. (2011b). "Definition of seismic input for out-of-plane response of masonry walls: II. Formulation." *Journal of Earthquake Engineering*, 15(2), 195–213.

Moon, L., Dizhur, D., Senaldi, I., Derakhshan, H., Griffith, M., Magenes, G., and Ingham, J. (2014). "The demise of the URM building stock in Christchurch during the 2010–2011 Canterbury earthquake sequence." *Earthquake Spectra*, 30(1), 253–276.

Penner, O. (2014). "Out-of-plane dynamic stability of unreinforced masonry walls connected to flexible diaphragms." Ph.D. thesis, University of British Columbia, Canada.

Penner, O. and Elwood, K. (2015). "Out-of-plane dynamic stability of unreinforced masonry walls: shake table study." *Earthquake Spectra*, xx(xx), xx–xx.

Sharif, I., Meisl, C., and Elwood, K. (2007). "Assessment of ASCE 41 height-to-thickness ratio limits for URM walls." *Earthquake Spectra*, 23(4), 893–908.

Sorrentino, L., Masiani, R., and Griffith, M. C. (2008). "The vertical spanning strip wall as a coupled rocking rigid body assembly." *Structural Engineering and Mechanics*, 29(4), 433–453.

Tena-Colunga, A. and Abrams, D. P. (1995). "Simplified 3-d dynamic analysis of structures with flexible diaphragms." *Earthquake engineering & structural dynamics*, 24(2), 221–232.

Wilhelm, M., Mojsilovic, N., and Dazio, A. (2007). "Out-of-plane shaking table tests on unreinforced masonry walls." *10th North American Masonry Conference*, 671–682.

Wilson, A. (2012). "Seismic assessment of timber floor diaphragms in unreinforced masonry buildings." Ph.D. thesis, University of Auckland, New Zealand.

TABLE 1: Model parameter formulations and reference values

	Parameter	Reference value	Description/Formulation
Input	t	330 mm	wall thickness
	h/t	11	slenderness ratio
	L	1.0 m	wall length
	ρ	2100 kg/m^3	wall density
	h_{cr}	0.6	relative crack height
	s_v	12 mm	joint thickness
	s_h	10 mm	spall depth
	ζ_t, ζ_b	0.05	damping ratio, top & bottom
	T_t, T_b	1.0 s	period, top & bottom
	R_{M_t}, R_{M_b}	3.0	mass ratio, top & bottom
	p	0 kN/m	axial load per unit length
Derived	h	3.63 m	$t \cdot (h/t)$
	h_t	1.452 m	$h \cdot (1 - h_{cr})$
	h_b	2.178 m	$h \cdot h_{cr}$
	M_w	2516 kg	$\rho \cdot h \cdot t \cdot L$
	M_{w_t}	1006 kg	$M_w \cdot (1 - h_{cr})$
	M_{w_b}	1510 kg	$M_w \cdot h_{cr}$
	M_{d_t}, M_{d_b}	3773 kg	$R_{M_{t,b}} \cdot \frac{M_w}{2}$
	k_t, k_b	199 kN/m	$\left(\frac{2\pi}{T_{t,b}}\right)^2 \cdot \left(\frac{M_w}{2} + M_{d_{t,b}}\right)$
	c_t, c_b	3160 N s/m	$\zeta_{t,b} \cdot 2\sqrt{k_{t,b} \cdot \left(\frac{M_w}{2} + M_{d_{t,b}}\right)}$

TABLE 2: Exposure factor

		C_e	
Exposure	P_{col}	Stiff	Flexible
very high	5%	0.9	0.9
high	10%	1.0	1.0
low	20%	1.15	1.1
very low	50%	1.5	1.25

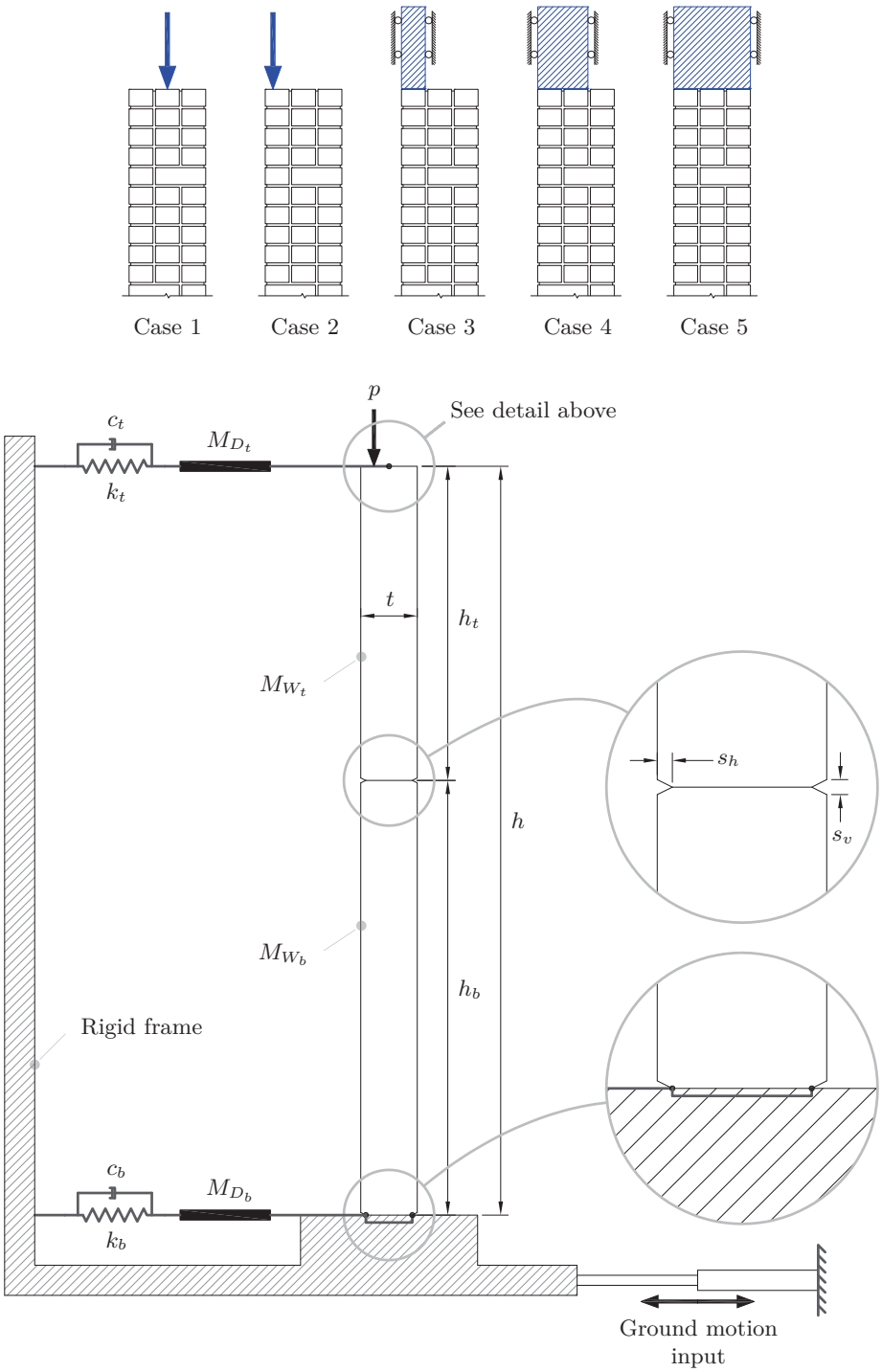

FIG. 1: Model configuration (see Table 1 for model parameter definitions)

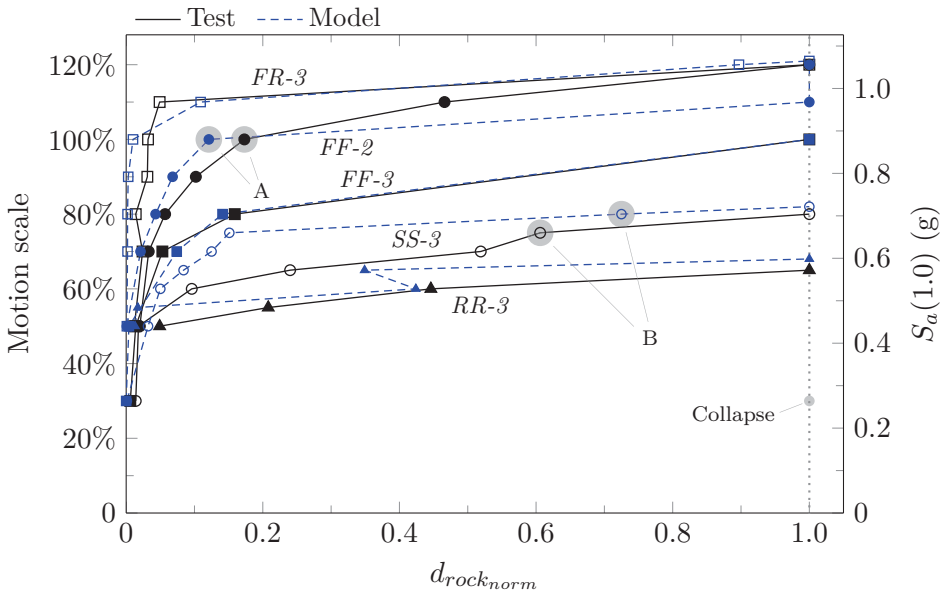

FIG. 2: Modelled vs. tested peak rocking displacements

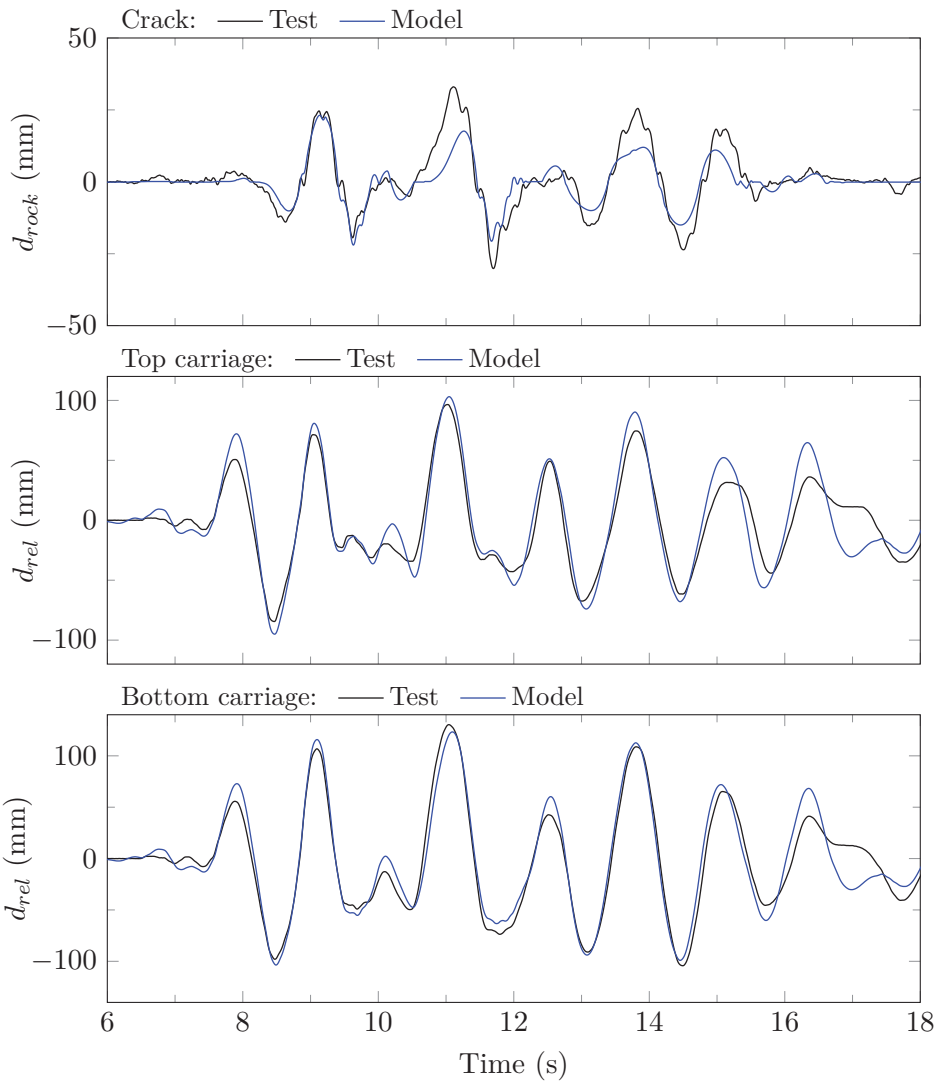

FIG. 3: Modelled vs. tested displacement time histories, wall *FF-2*, run 9

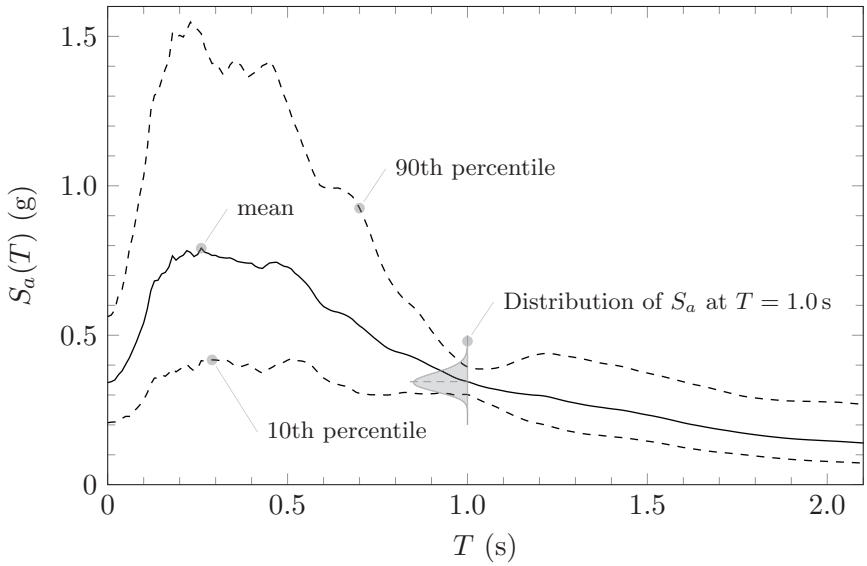

FIG. 4: S_a at collapse for the reference configuration

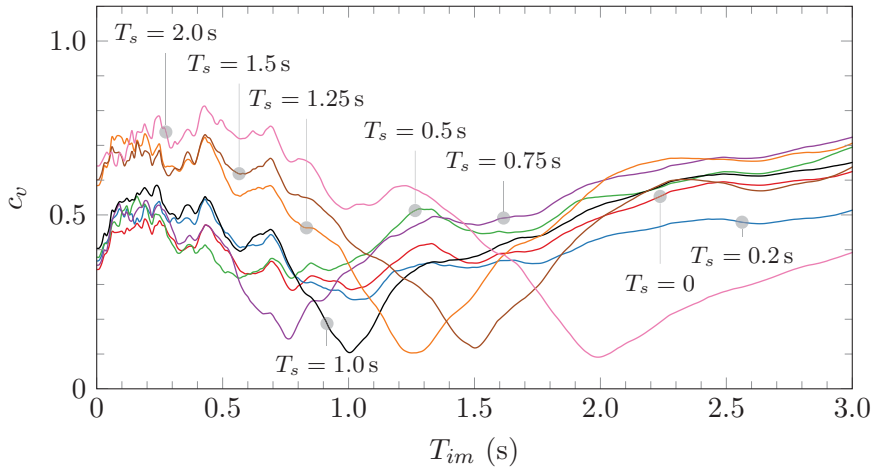

FIG. 5: Coefficient of variation c_v, for varying period T_{im} at which the intensity measure S_a is evaluated for varying wall-diaphragm system period T_s

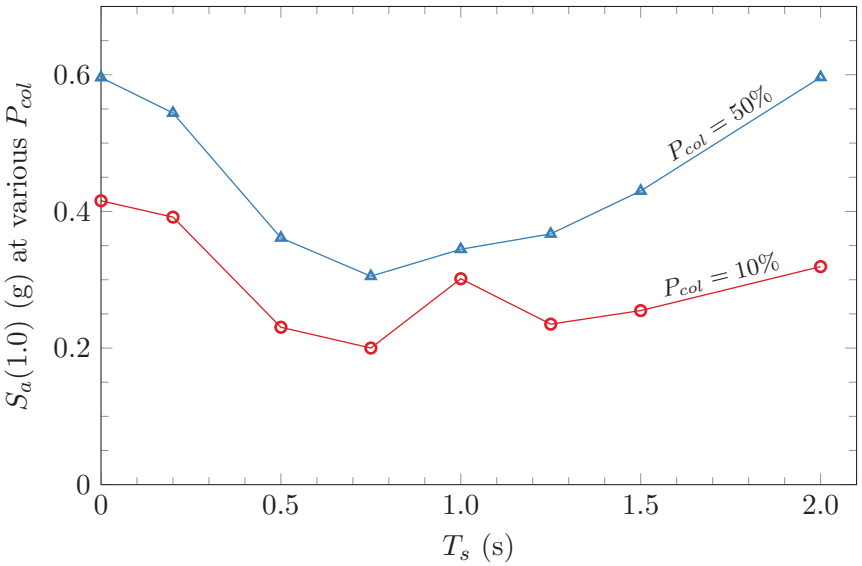

FIG. 6: Constant P_{col} points, varying period

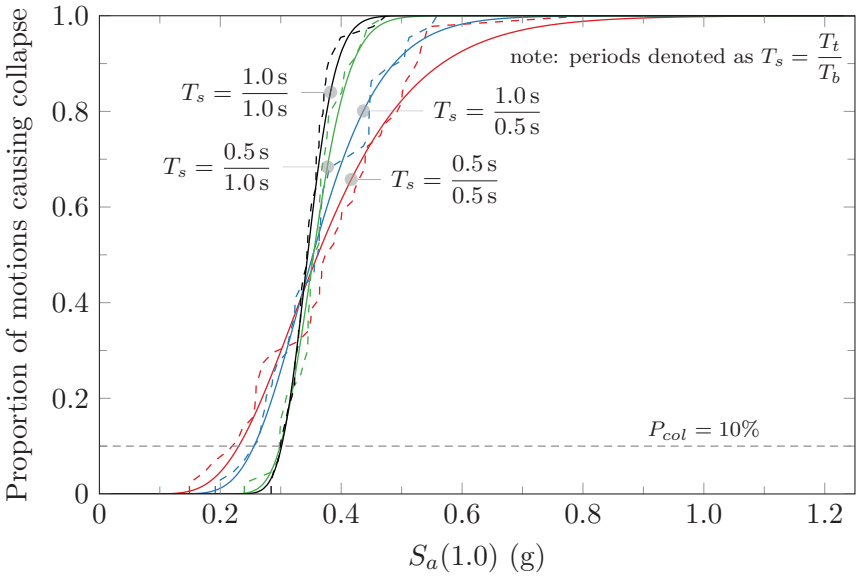

FIG. 7: Fragility curves, $T_s = 0.5$ and $1.0\,\text{s}$ combinations

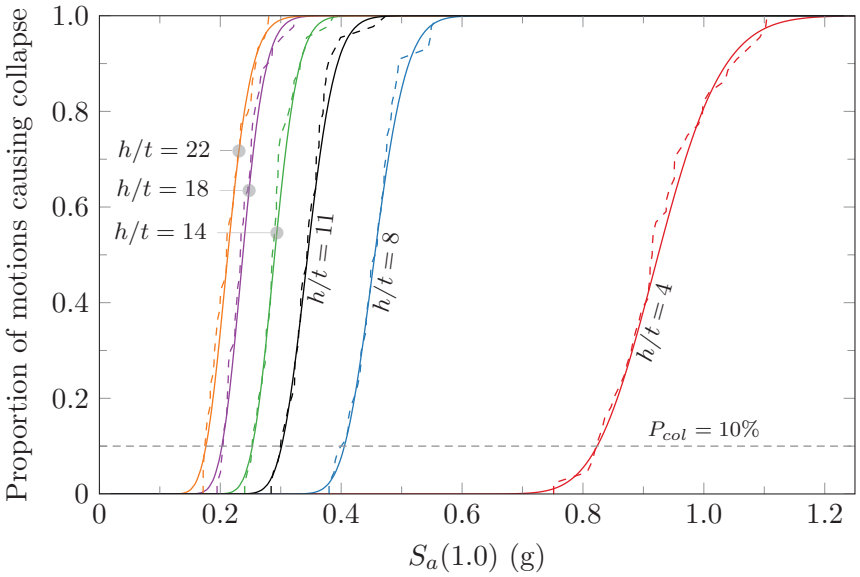

FIG. 8: Fragility curves, varying slenderness

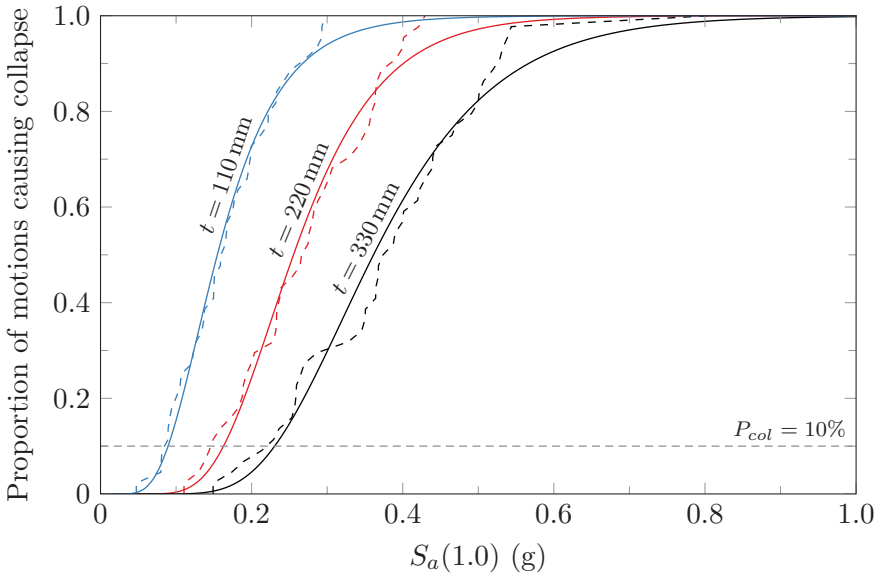

FIG. 9: Fragility curves, varying thickness, $T_s = 0.5\,\mathrm{s}$

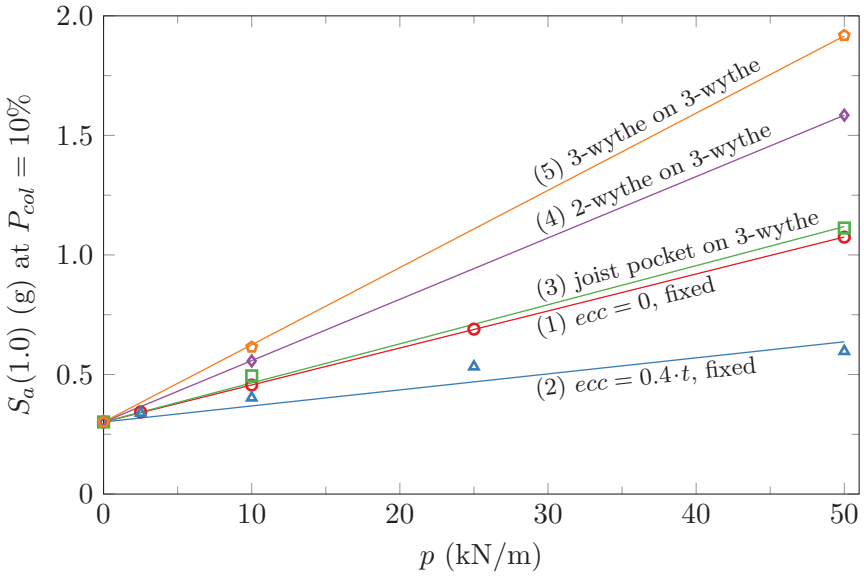

FIG. 10: S_a for $P_{col} = 10\,\%$, varying p and boundary conditions

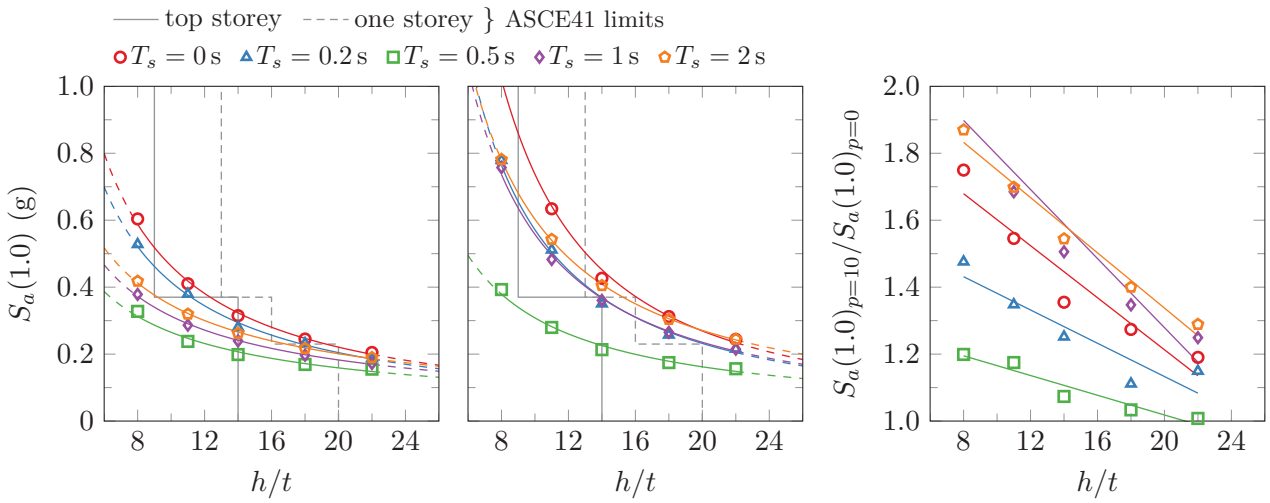

(a) $p = 0$ (b) $p = 10\,\mathrm{kN/m}$ (c) Ratio

FIG. 11: S_a for $P_{col} = 10\,\%$, varying period

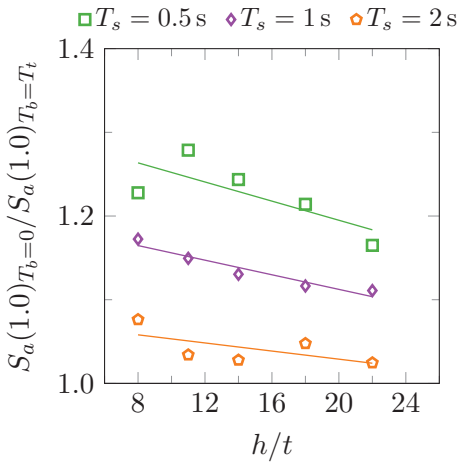

FIG. 12: Relative stability increase due to rigid bottom diaphragm

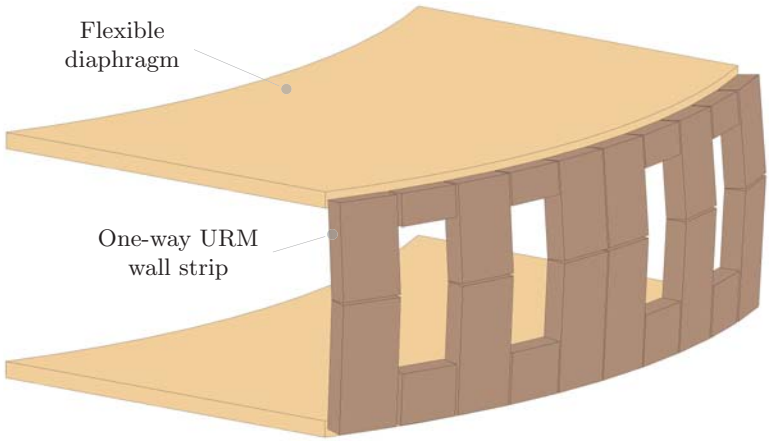

FIG. 13: Wall response along the length of a flexible diaphragm

FIG. 14: Out-of-plane wall failure, Christchurch 2011 (credit: D. Dizhur)

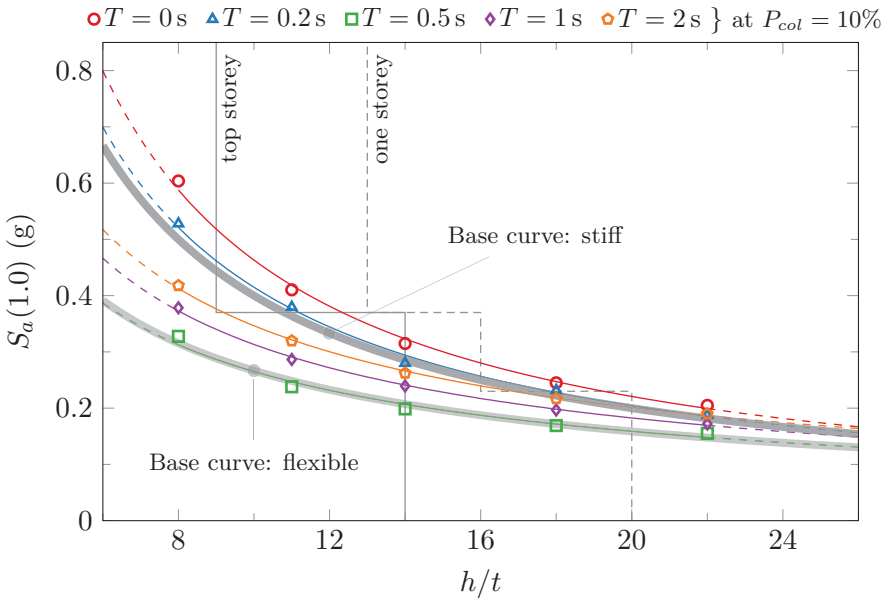

FIG. 15: Base curves, for 3-wythe wall, no axial load, high exposure, upper storey

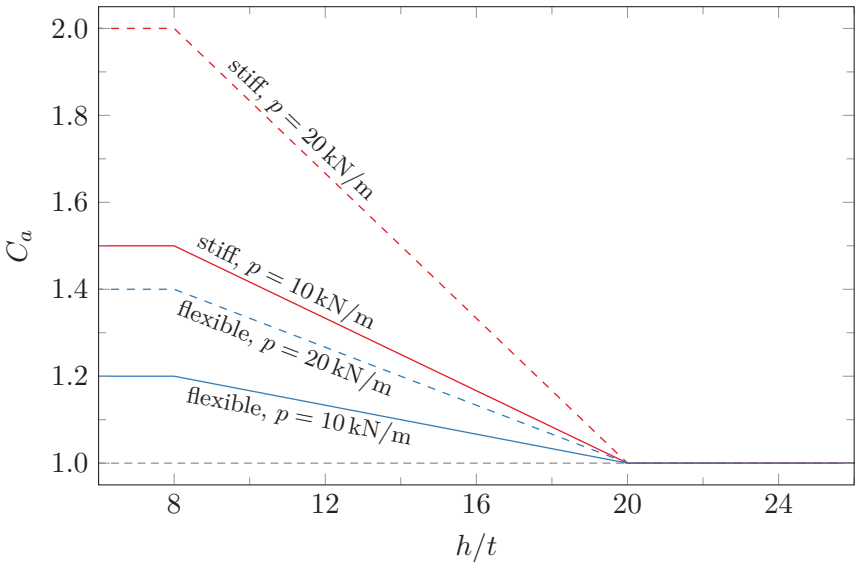

FIG. 16: Axial load correction factors

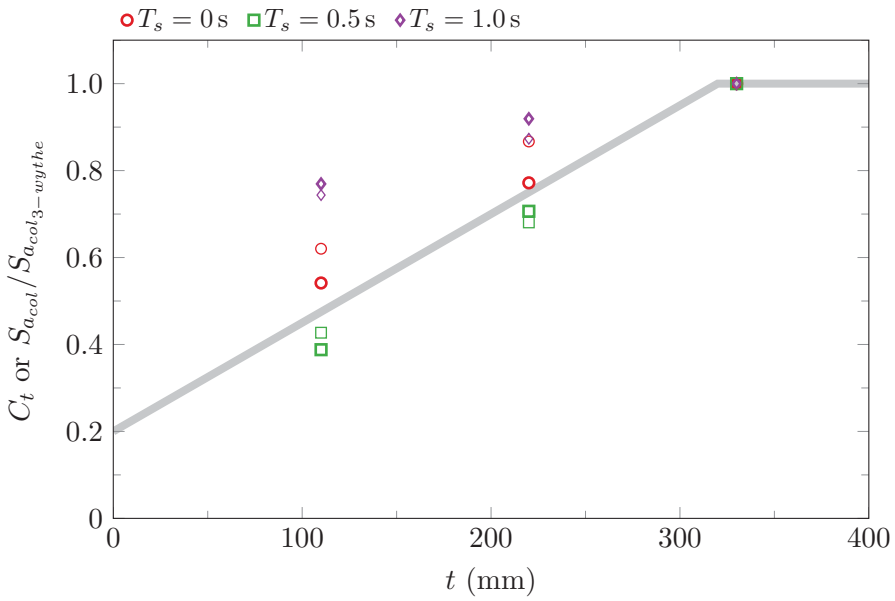

FIG. 17: Thickness correction factors, compared to model results at $P_{col} = 10\,\%$

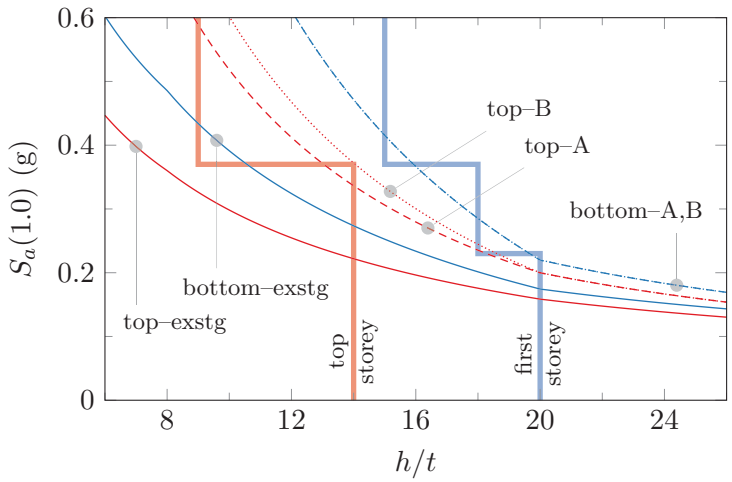

FIG. 18: Example assessment curves